International Journal of Agricultural Technology 2026 Vol. 22(3):1195-1214
DOI: https://doi.org/10.63369/ijat.2026.22.3.1195-1214
Available online http://www.ijat-aatsea.com
ISSN 2630-0192 (Online)

Dorsal fin morphology and phylogenetic insights in bamboo sharks (*Chiloscyllium* spp.)

Laongdee, P.[1], Krajangdara, T.[2], Senanan, W.[3], Khudamrongsawat, J.[4], Panithanarak, T.[5], Karuwancharoen, R.[5] and Klangnurak, W.[1*]

[1]Aquacultural Technology and Aquatic Resource Management, School of Agricultural Technology, King Mongkut's Institute of Technology Ladkrabang, Bangkok 10520, Thailand; [2]66/27 Thepthanee Village, Rassada, Muang, Phuket 83000, Thailand; [3]Department of Aquatic Science, Faculty of Science, Burapha University, Chonburi 20131, Thailand; [4]Department of Biology, Faculty of Science, Mahidol University, Bangkok 10400, Thailand; [5]Institute of Marine Science, Burapha University, Chonburi 20131, Thailand.

Laongdee, P., Krajangdara, T., Senanan, W., Khudamrongsawat, J., Panithanarak, T., Karuwancharoen, R. and Klangnurak, W. (2026). Dorsal fin morphology and phylogenetic insights in bamboo sharks (*Chiloscyllium* spp.). International Journal of Agricultural Technology 22(3):1195-1214.

Abstract Two closely related species, *C. hasseltii* and *C. griseum*, showed overlapping shape variations in their first dorsal fins. However, the proportions of the first dorsal fin height/total length and the first dorsal fin inner margin/total length were observed to be significantly different between these two species. This difference can be integrated into the dichotomous key for *Chiloscyllium*. Phylogenetic analysis based on the cytochrome c oxidase I (*COI*) gene was consistent with the morphology of the first dorsal fin, indicating that *C. punctatum* differs from other *Chiloscyllium* species. However, phylogenetic tree based on the NADH dehydrogenase 2 (*ND2)* gene fragments grouped the clade of *C. punctatum* with other clades of *Chiloscyllium*. Most *Chiloscyllium* species formed monophyletic groups based on the two gene fragments, except for *C. hasseltii* and *C. griseum*, which clustered together. This research provides practical knowledge for field-based species identification and accurate classification within the genus *Chiloscyllium*, enhances our understanding of its phylogenetic relationships, and supports the future development of a field guide.

Keywords: Dorsal fin, Geomorphometry, Morphometry, Evolution

Introduction

A large portion of shark populations is severely threatened by overfishing, leading to biodiversity loss and potential ecosystem collapse (Dulvy *et al.*, 2021). Since some species are more vulnerable than others, the lack of accurate species identification may contribute to the endangerment of certain shark species. Field

[*] **Corresponding Author:** Klangnurak, W.; **Email:** wanlada.kl@kmitl.ac.th

monitoring is therefore essential for assessing shark biodiversity. However, identifying cryptic species is particularly challenging for non-taxonomists, as many exhibit similar morphological characteristics. Thus, key morphological features play a crucial role in accurate biodiversity assessments, education, and environmental literacy. In this study, we focus on bamboo sharks, or longtailed carpet sharks (Order Orectolobiformes, Family Hemiscylliidae, Genus *Chiloscyllium*), found in Thai waters, as a case study for identifying similar-looking species using morphological characteristics.

These sharks are distributed in estuaries, coastlines, coral reefs, and oceans in the Indo-West Pacific Ocean (Compagno, 2001). There are eight species worldwide (Compagno, 2001; Dingerkus and DeFino, 1983; Weigmann, 2016), but only five have been reported in Thailand: *Chiloscyllium punctatum*, *C. hasseltii, C. griseum*, *C. plagiosum*, and *C. indicum* (Krajangdara *et al.*, 2022). Sharks of this genus are commonly targeted and caught as bycatch using trawls, gillnets, longlines, and handline fisheries, both industrially and artisanally, for their meat and fins in Southeast Asia (Arai and Azri, 2019; Arunrugstichai *et al.*, 2018; Dharmadi and Satria, 2015; DoA, 2009; Klangnurak *et al.*, 2023; SEAFDEC, 2017). This bycatch has led to their decline in population, with *C. hasseltii* classified as endangered (EN) and *C. griseum*, *C. burmensis*, and *C. indicum* classified as vulnerable (VU) according to the IUCN Red List (IUCN, 2024).

The first dorsal fin, a major ingredient of shark fin soup, has been used for species identification within the genus *Chiloscyllium* (Dingerkus and DeFino, 1983). However, studies on the morphological structure and function of the dorsal fin are limited compared to extensive studies on pectoral fins, which have been conducted from multiple perspectives, including illustrations on how structural changes develop in response to environmental pressures and habitat (Cole and Currie, 2007; Hoffmann *et al.*, 2020; Sternes *et al.*, 2024; Wilga and Lauder, 2001).

The integration of morphological and genetic data is essential for evolutionary studies. Morphology provides insights into structural adaptations influenced by environmental pressures, whereas genetic analysis reveals molecular differences and evolutionary relationships among species. The phylogenetic relationships of *Chiloscyllium* have been investigated using *COI* gene sequences from public databases and sequences from other shark orders (Vélez-Zuazo and Agnarsson, 2011). Further analysis has been conducted using two additional gene markers, mitochondrially encoded 12S ribosomal RNA (*12S rRNA)* and cytochrome b (*Cytb*) (Masstor *et al.*, 2014), to reveal the differences in tree topology, possibly because of the use of distinct genetic markers and species samples. However, these previous studies did not integrate

morphological characteristics to understand the phylogenetic relationships within this genus.

The objectives of this study were to examine variations in dorsal fin morphology and morphometrics among bamboo sharks (*Chiloscyllium* spp.) found in Thailand, apply molecular markers to distinguish morphologically similar species, and enhance the understanding of phylogenetic relationships within the genus *Chiloscyllium*.

Materials and methods

Samples collected and species identification

Samples of *Chiloscyllium* spp. were collected by local fishermen and researchers from the Department of Fisheries, Thailand, between February 2022 and December 2023 from both the Gulf of Thailand (Chanthaburi, Rayong, Chonburi, Songkhla, and Pattani provinces) and the Andaman Sea (Ranong, Phuket, Trang, and Satun provinces) (Figure 1). Samples were identified at the species level following the method of Krajangdara*, et al.* (2022). Four of the five species of *Chiloscyllium* previously recorded in Thai waters were among those collected, with the exception of *C. plagiosum*. All the specimens were stored in a freezer at -40˚C prior to morphological analysis. Fin tissues were clipped and stored in 95% ethanol prior to DNA analysis. Unfortunately, owing to tissue degradation, only three samples of each species from the Rayong, Songkhla, Ranong, Phuket, Trang, and Satun provinces were used for DNA analysis. Some specimens were subjected to both morphological and DNA analyses.

Morphological analyses of fin

C. hasseltii (n = 25), *C. griseum* (n = 8), *C. punctatum* (n = 37), and *C. indicum* (n = 22) were used for the geometric morphometric analysis of the first dorsal fin. The first dorsal fin was photographed using a digital camera (DSLR NIKON D5300; Nikon, Thailand) equipped with an AF-S DX NIKKOR 18–55 mm f/3.5–5.6G VR II lens. The photos were transferred to TPS. files using tpsUtil64 version 1.82 software (Rohlf, 2021b). All the 20 landmarks around the fin, based on Cooper *et al.* (2020), were spotted using tpsDig2 version 2.32 software (Rohlf, 2021a) (Figure 2A). The raw landmark file data from tpsDig2 were input into MorphoJ 1.07a software (Klingenberg, 2011) to identify variations in shape. Canonical Variate Analysis (CVA) was performed to display the variation in first dorsal fin shape among species and then provide a scatter plot of specimens along the first two canonical axes using MorphoJ 1.07a

software (Klingenberg, 2011). Goodall's F-test of Procrustes coordinates or Procrustes ANOVA was used to assess morphological differences in the first dorsal fin among species. Pairwise Procrustes distances were calculated to assess the shape differences between species. Both Procrustes ANOVA and Procrustes distances were computed using the MorphoJ 1.07a software (Klingenberg, 2011).

Two species with similar fin shapes, *C. hasseltii* and *C. griseum* (n = 6), were used to perform additional morphometric analyses of the dorsal fins. Five morphometric characters of the first dorsal fin (Figure 2B), as reported by Weigmann (2012): first dorsal fin base (D1B), first dorsal fin anterior margin (D1A), first dorsal fin height (D1H), first dorsal fin posterior margin (D1P), first dorsal fin inner margin (D1I), and total length (Figure 2C) were measured. Five dorsal fin traits were normalized to the total length (TL) and reported as a percentage of the total length. An independent samples t-test was conducted to evaluate differences in the morphometric proportions between the two species using SPSS v.28 (Elliott and Woodward, 2014).

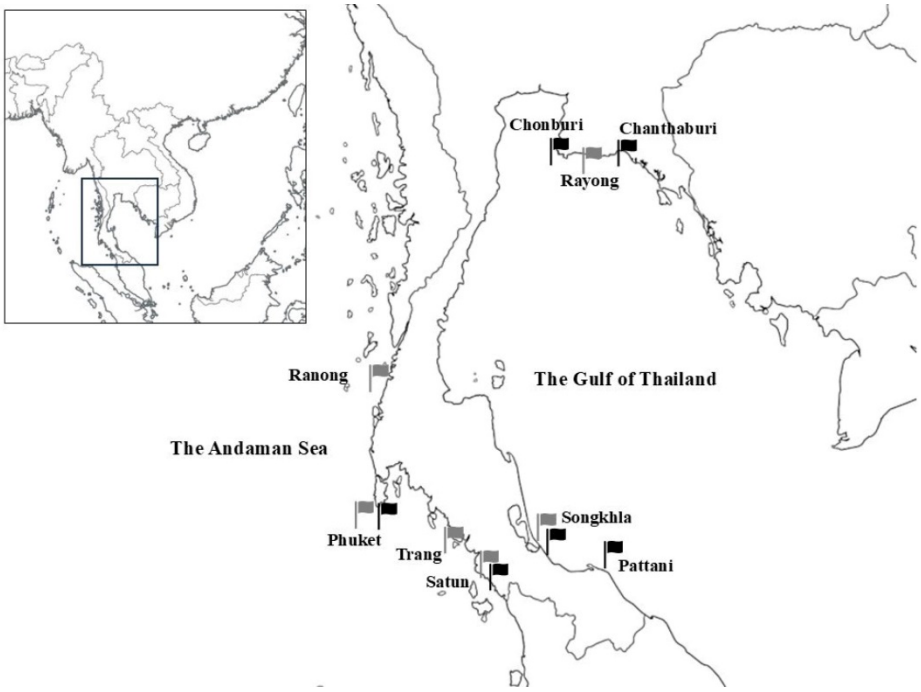

Figure 1. Sampling locations for morphological analysis of the first dorsal fin in six provinces (dark icons) and molecular study in six provinces (light icons) in Thai waters

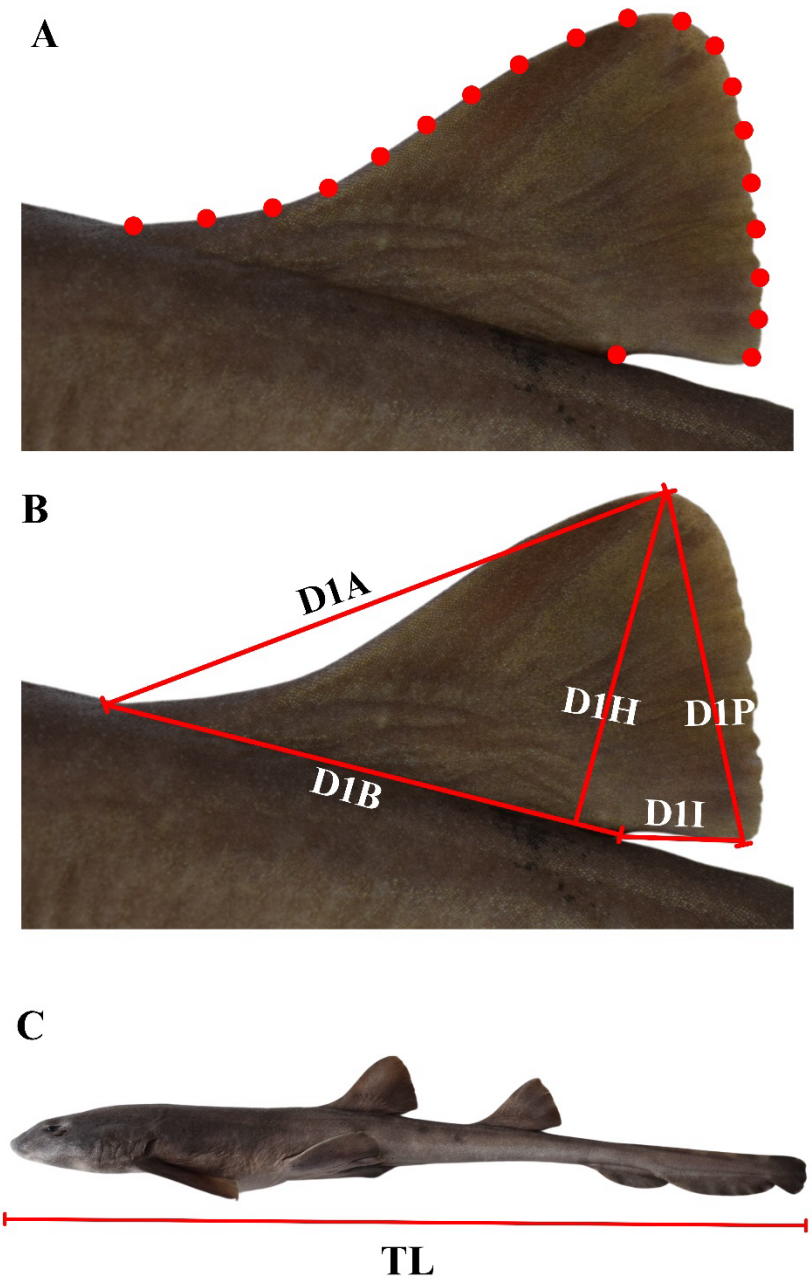

Figure 2. Morphological characters recorded for geomorphometric and morphometric studies: The twenty landmarks of the first dorsal fin for morphometrics (A), five characteristics for morphometric study of *C. hasseltii* and *C. griseum* (B), and total length (TL) (C)

Molecular examination and analysis

The genomic DNA was extracted from specimens of *C. hasseltii* (n = 3), *C. griseum* (n = 3), *C. punctatum* (n = 3), and *C. indicum* (n = 3). Approximately 0.5 cm² of tissue was processed using the phenol-chloroform method (Sambrook *et al.*, 1989) or 1 mg of tissue was extracted using Qiagen® DNeasy Blood & Tissue Kits (Qiagen, California, USA), in accordance with the manufacturer's protocol. The *COI* and *ND2* genes were amplified and sequenced. A partial sequence of the *COI* gene was amplified via Polymerase Chain Reaction (PCR) using the FishF1 (5′- TCA ACC AAC CAC AAA GAC ATT GGC AC -3′) and FishR1 primers (5′- TAG ACT TCT GGG TGG CCA AAG AAT CA -3′) (Ward *et al.*, 2005). PCR amplification was conducted in 20 µl volume containing PCR buffer (10X) 2 µl, dNTPs (2.5 mmol/µl) 2 µl, $MgCl_2$ (2.5 mmol/µl) 2 µl, i-Taq™ DNA Polymerase (5U/µl) 0.2 µl (Intron, Korea), 0.5–1 µl of 10 pmol/µl of each primer, 1–2 µl of genomic DNA template, and completed with ddH_2O. The thermocycler conditions were as follows: initial denaturation for 2 min at 95 ˚C, followed by 35 cycles of amplification (30 s at 94 ˚C, 30 s at 54 ˚C, and 1 min at 72 ˚C), and a final extension step of 10 min 72˚C. The partial sequence of *ND2* gene was amplified via PCR using the ILEM (5′- AAG GAC CAC TTT GAT AGA GT -3′) and ASNM primers (5′- AAC GCT TAG CTG TTA ATT AA -3′) (Naylor *et al.*, 2012). PCR amplification was conducted in 20 µl volume containing PCR buffer (10X) 2 µl, dNTPs (2.5 mmol/µl) 2 µl, $MgCl_2$ (2.5 mmol/µl) 2 µl, i-Taq™ DNA Polymerase (5U/µl) 0.2 µl (Intron, Korea), 0.5–1 µl of 10 pmol/µl of each primer, 1–2 µl of genomic DNA template, and completed with ddH_2O. The thermocycler conditions were as follows: initial denaturation for 2 mins at 94 ˚C, followed by 35 cycles of amplification (20 s at 94 ˚C, 20 s at 52 ˚C, and 1 min at 65 ˚C), and a final extension step of 3 min 72 ˚C. All PCR products were checked via electrophoresis on 1.5% agarose gel with RedSafe Nucleic Acid Stain. PCR products were purified and sequenced by U2Bio Co., Ltd. (Thailand) and Gibthai Co., Ltd. (Thailand).

Molecular markers were employed to distinguish morphologically similar species. The sequences were visualized and trimmed using CodonCode Aligner (Richterich, 2004). A total of 12 *COI* fragments with the length of 412 bp was obtained from *C. hasseltii* (n = 3), *C. griseum* (n = 3), *C. punctatum* (n = 3), and *C. indicum* (n = 3), whereas 10 *ND2* fragments of 605 bp from *C. hasseltii* (n =1), *C. griseum* (n = 3), *C. punctatum* (n = 3), and *C. indicum* (n = 3) were successfully sequenced. All sequences were analyzed using the Basic Local Alignment Search Tool (BLAST: https://blast.ncbi.nlm.nih.gov/Blast.cgi) in the GenBank database (Altschul *et al.*, 1997) and the Barcode of Life Data System (BOLD: https://v3.boldsystems.org/index.php/databases) to identify them at the

lowest taxonomic level, considering the highest percentage similarity with reference sequences in the database. After the sequence similarity search, all the sequences were submitted to the NCBI database.

Phylogenetic relationships among *Chiloscyllium* species were examined using nucleotide sequences from both the NCBI database and this study. Twenty-four sequences of the *COI* gene and seventeen sequences of the *ND2* gene were downloaded from the NCBI database. *Stegostoma tigrinum* was selected as an outgroup. Multiple sequences were aligned using ClustalW software. The most suitable models for constructing the phylogenetic tree using MEGA11 (Tamura *et al.*, 2021) were the TrN+G model for the *COI* sequences and the HKY+I model for the *ND2* sequences. A maximum-likelihood phylogenetic tree was constructed with 1000 bootstrap replications. The morphology of the fin in this study, combined with other characteristics such as body color and ridges from the literature review, was used to explain the phylogenetic relationships.

Results

Morphological analyses

Immature and mature samples of *C. punctatum* (55.8–86.2 cm TL), *C. hasseltii* (40.2–72.2 cm TL), *C. griseum* (51.7–64 cm TL), and *C. indicum* (39.4–55.3 cm TL) were used for geometric morphometric analysis. The CVA of the 20 landmarks on the first dorsal fin showed a strong tendency to differentiate the samples into three groups (Figure 3). *C. punctatum* and *C. indicum* were strongly separated, whereas *C. griseum* and *C. hasseltii* mostly overlapped. The first two canonical axes showed most of the total variance (74.8%). Positive scores for CV1 were mainly for *C. indicum*, which has a slender, elongated shape with a straight trailing edge (Figure 4). *C. punctatum* was the only species with negative CV2 scores, displaying a clear vertical height and a concave trailing edge. *C. griseum* and *C. hasseltii* mostly overlapped and had negative scores for CV1, exhibiting a shorter shape but greater posterior fin height than the other groups and with a trailing edge that ranged from slightly convex in *C. griseum* to straight in *C. hasseltii*. Based on shape change, Procrustes ANOVA showed highly significant differences among the species (Shape: $F = 11.48$, $df = 144$, $P < 0.001$; centroid size: $F = 20.39$, $df = 4$, $P < 0.001$). The greatest pairwise differentiation between species based on Procrustes distances, which infer shape differentiation, was in the comparison between *C. punctatum* and *C. indicum* (Procrustes distance = 0.1240, $P < 0.0001$), followed by the comparison between *C. indicum* and *C. hasseltii* (Procrustes distance = 0.1042, $P < 0.0001$).

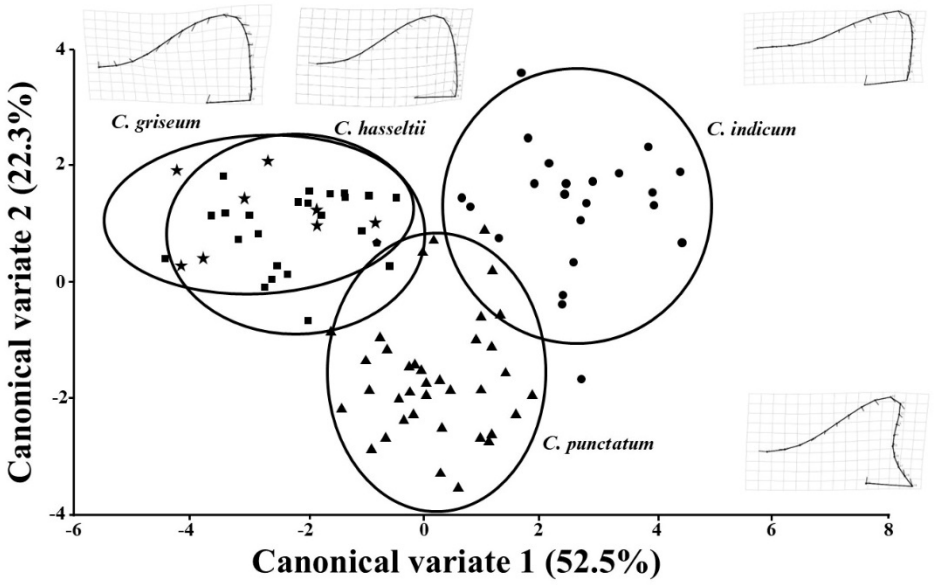

Figure 3. Canonical variate analysis (CVA) of the first dorsal fin morphology in *C. punctatum*, *C. hasseltii*, *C. griseum*, and *C. indicum* based on geomorphometric data

Five additional characters of *C. hasseltii* and *C. griseum*, which show undifferentiated fin shapes based on geometric morphometric analysis, were investigated. Two of these five morphometric proportions showed significant differences between the two species. The first characteristic was the height of the first dorsal fin (D1H), normalized by total length (TL), and it showed a significant difference (T = -2.966, df = 14, P = 0.005) (Table 1). The measurement of D1H/TL as a percentage was 7.88 ± 0.8% for *C. hasseltii* and 8.42 ± 0.4% for *C. griseum*, making the dorsal fin of *C. hasseltii* to be approximately 0.94 times flatter than that of *C. griseum*. The other characteristic was the inner margin of the first dorsal fin (D1I), normalized by TL (T = -2.776, df = 14, P = 0.007). The measurement of D1H/TL as a percentage was 2.95 ± 0.3% for *C. hasseltii* and 3.46 ± 0.5% for *C. griseum*, suggesting that the inner margin of the dorsal fin in *C. hasseltii* was approximately 0.85 times the length of that in *C. griseum*.

Dorsal fin morphology and phylogenetic relationships

Dorsal fin morphology was consistent with the phylogenetic trees. Based on both trees, most of the examined species, except *C. punctatum*, had a straight

trailing edge of the first dorsal fin. *C. punctatum*, which appears as a basal group of *Chiloscyllium*, based on the *COI* gene, was the only species with a concave trailing edge. Within the group of species with a straight trailing edge on the first dorsal fin, *C. hasseltii* and *C. griseum* showed a short fin shape but greater posterior fin height, similar to *C. arabicum* and *C. burmensis*. The dorsal fins of *C. plagiosum* and *C. indicum* were slender and elongated in shape (Figure 3, 4).

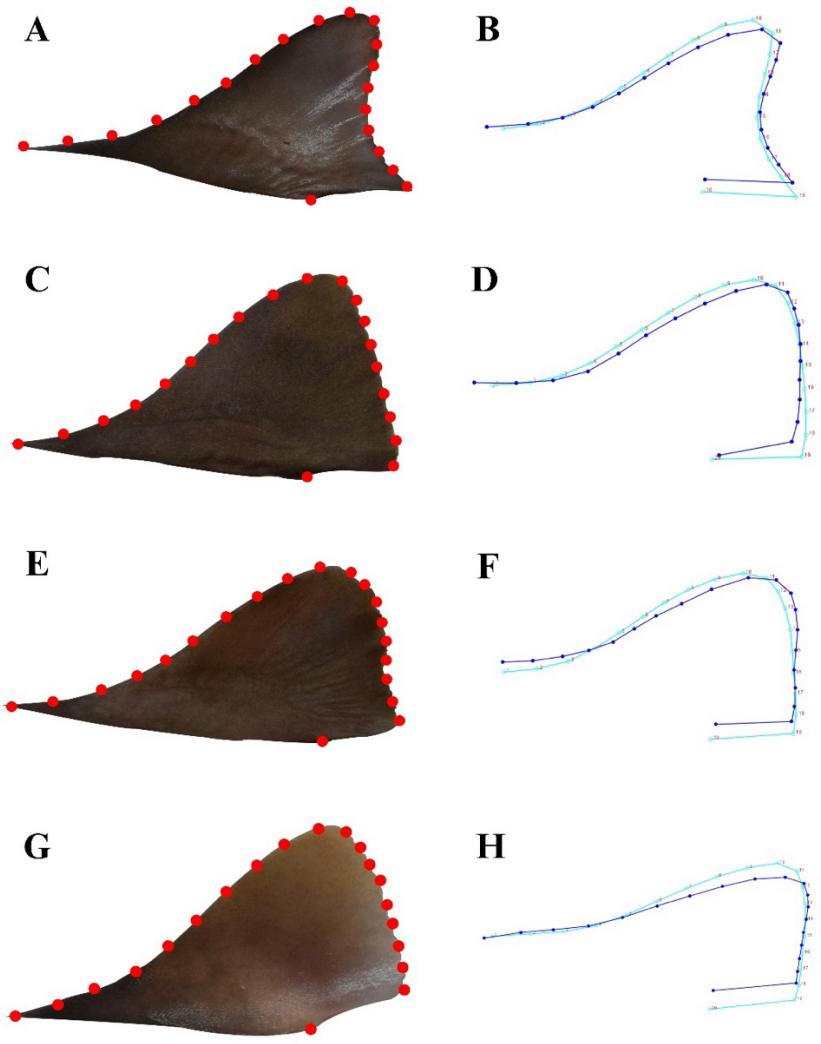

Figure 4. Landmarks of the first dorsal fin of *C. punctatum* (A, B), *C. hasseltii* (C, D), *C. griseum* (E, F), and *C. indicum* (G, H) in variation analysis: The light blue line referred to the model fin shape, and the dark blue line represented the average fin shape of each species

Genetic examination and phylogenetic analyses

Samples were labeled based on their morphological identification and confirmed using BLAST and BOLD analyses (Table 2 and Table 3), which showed 100% genetic similarity to the reference sequences of *C. indicum* and *C. punctatum*, respectively. However, genetic analyses of *C. hasseltii* and *C. griseum* revealed ambiguous results, with the highest similarity percentages corresponding to multiple species and leading to unclear species identification. Based on the *COI* gene, the morphologically identified *C. griseum* was assigned to both *C. griseum* and *C. hasseltii* (Table 2), whereas the *ND2* gene clearly identified it as *C. griseum* (Table 3). Morphologically identified *C. hasseltii* matched with *C. hasseltii* and *C. griseum* by both genetic markers.

Phylogenetic trees based on *COI* gene revealed five clades of *Chiloscyllium* (Clades A–E; Figure 5). Clade A, with 94% bootstrap support, included two subclades, one containing only *C. griseum* from India and Sri Lanka and the other containing both *C. hasseltii* and *C. griseum* from this study. Clade B, the sister clade of Clade A, contained *C. arabicum* and *C. burmensis* with each species forming its own subclade. Clade C, which showed the grouping of *C. plagiosum*, was sister to Clade D, which contains only *C. indicum*. Finally, Clade E, which was basal to all the clades, was a monophyletic group of *C. punctatum*.

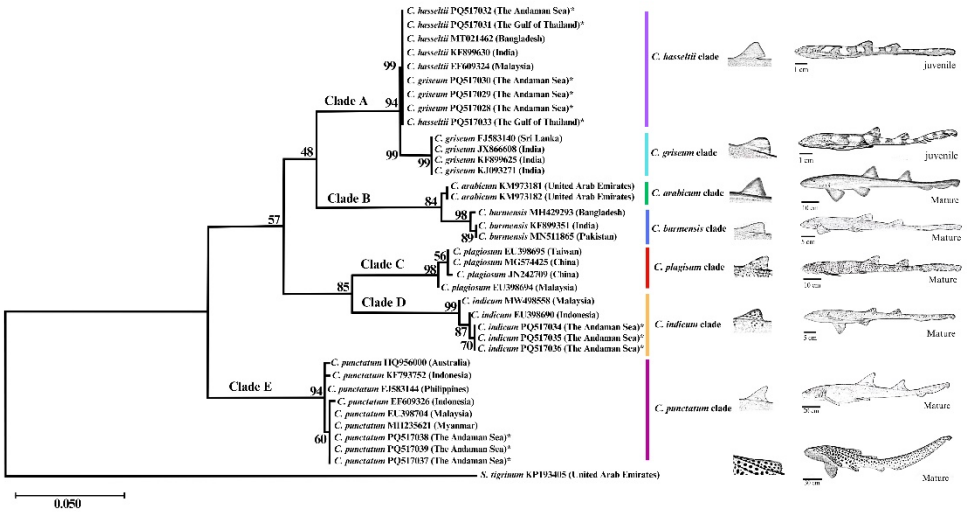

Figure 5. Phylogenetic relationship within the genus *Chiloscyllium*, using *COI* sequences, with details of species, GenBank accession numbers, and geographic origin; The samples collected in Thailand are shown in asterisk

Phylogenetic analysis of the *ND2* gene revealed a distinct tree topology compared to that of the *COI* phylogenetic tree (Clades A–E; Figure 6). Clade A, with 100% bootstrap support, included one branch containing *C. griseum* from the populations in this study and Sri Lanka, as well as *C. hasseltii* from this study and Indonesia. In Clade B, *C. griseum* from India formed a monophyletic group with *C. arabicum* from Iran. Clade C, which contained *C. indicum*, was a sister clade to Clade D (*C. plagiosum*). Clade E is a monophyletic group of *C. punctatum*.

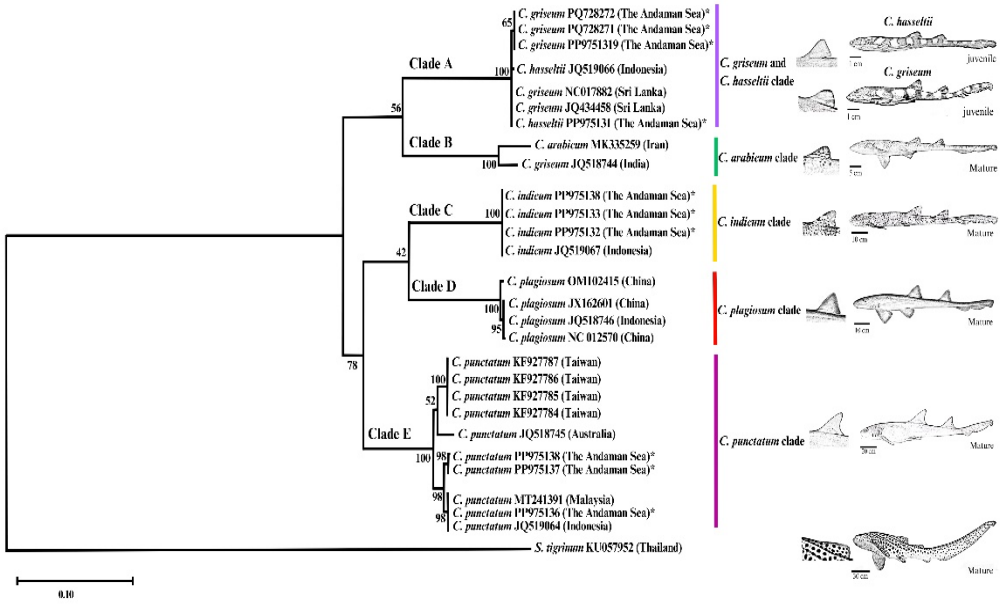

Figure 6. Phylogenetic relationship within the genus *Chiloscyllium*, using *ND2* sequences, with details of species, GenBank accession numbers, and geographic origin; The samples collected in Thailand are shown in asterisk

Table 1. Morphometric characteristics of the first dorsal fin of *C. hasseltii* and *C. griseum*

Characteristics	*C. hasseltii* (n = 10)		*C. griseum* (n = 6)		T-Test		
	Range	Average ± SD	Range	Average ± SD	t	df	p-value
First dorsal fin base (D1B) / TL (%)	8.32–10.51	9.59 ± 0.7	9.12–9.89	9.37 ± 0.3	0.726	14	0.240
First dorsal fin anterior margin (D1A) / TL (%)	10.95–13.05	12.12 ± 0.8	11.59–13.31	12.30 ± 0.6	-0.464	14	0.325
First dorsal fin height (D1H) / TL (%)	5.93–9.06	7.88 ± 0.8	8.25–8.99	8.42 ± 0.4	-2.966	14	0.005
First dorsal fin posterior margin (D1P) / TL (%)	5.67–7.99	6.95 ± 0.7	6.44–7.67	7.03 ± 0.5	-0.236	14	0.409
First dorsal fin inner margin (D1I) / TL (%)	2.62–3.62	2.95 ± 0.3	2.88–4.19	3.46 ± 0.5	-2.776	14	0.007
First dorsal fin base (D1B)	37–62	50.5 ± 8.8	52–59	56.83 ± 2.8			
First dorsal fin anterior margin (D1A)	43–77	64.1 ± 11.9	69–80	74.5 ± 4			
First dorsal fin height (D1H)	23–51	41.7 ± 8.2	47–54	51 ± 2.8			
First dorsal fin posterior margin (D1P)	22–45	36.8 ± 7.6	37–48	42.67 ± 4			
First dorsal fin inner margin (D1I)	11–20	15.5 ± 2.7	18–26	21 ± 3.1			
Total length (TL)	388–590	525.7 ± 74.6	556–640	606.67 ± 34.7			

Table 2. Details of DNA sequence matches based on *COI* sequences from the NCBI and BOLD database

No.	Sample Code	Morphological Identification	Search Match	NCBI percent identity (%)	Query Cover (%)	NCBI Submission Accession No.	BOLD percent similarity (%)	BOLD Submission Accession No.
1	*C. griseum* PQ517028	*C. griseum*	*C. griseum*	100	100	KC175451	100	INELA027-12
			C. hasseltii	100	100	MF153995	100	FOAD568-05
2	*C. griseum* PQ517029	*C. griseum*	*C. griseum*	99.83	99	NC_017882	100	INELA027-12
			C. hasseltii	99.82	99	MN623878	100	FOAD568-05
3	*C. griseum* PQ517030	*C. griseum*	*C. griseum*	99.83	100	NC_017882	100	INELA027-12
			C. hasseltii	99.82	99	MN623878	100	FOAD568-05
4	*C. hasseltii* PQ517031	*C. hasseltii*	*C. hasseltii*	100	98	MF153997	100	FOAD568-05
			C. griseum	99.55	100	NC_017882	100	INELA027-12
5	*C. hasseltii* PQ517032	*C. hasseltii*	*C. hasseltii*	99.68	98	MN623878	99.84	JTF112-17
			C. griseum	99.52	100	NC_017882	99.84	INELA027-12
6	*C. hasseltii* PQ517033	*C. hasseltii*	*C. hasseltii*	99.84	99	MN623878	100	FOAD568-05
			C. griseum	99.84	99	NC_017882	100	INELA027-12
7	*C. indicum* PQ517034	*C. indicum*	*C. indicum*	100	97	EF609325	100	FOAE444-06
8	*C. indicum* PQ517035	*C. indicum*	*C. indicum*	100	100	EF609325	100	FOAE444-06

Table 2. Details of DNA sequence matches based on *COI* sequences from the NCBI and BOLD database (Continued)

No.	Sample Code	Morphological Identification	Search Match	NCBI percent identity (%)	Query Cover (%)	NCBI Submission Accession No.	BOLD percent similarity (%)	BOLD Submission Accession No.
9	*C. indicum* PQ517036	*C. indicum*	*C. indicum*	100	98	EF609325	100	-
10	*C. punctatum* PQ517037	*C. punctatum*	*C. punctatum*	98.98	99	AP019519	100	FOAD573-05
11	*C. punctatum* PQ517038	*C. punctatum*	*C. punctatum*	99.37	100	PQ047651	100	KERRI768-08
12	*C. punctatum* PQ517039	*C. punctatum*	*C. punctatum*	99.52	99	PQ047651	100	FOAD573-05

Table 3. Details of DNA sequence matches based on *ND2* sequences from the NCBI database

No.	Sample Code	Morphological Identification	Search Match	NCBI percent identity (%)	Query Cover (%)	NCBI Submission Accession No.
1	*C. griseum* PP975139	*C. griseum*	*C. griseum*	99.87	100	NC_017882
			C. hasseltii	99.87	100	PP975131
2	*C. griseum* PQ728271	*C. griseum*	*C. griseum*	99.88	100	NC_017882
			C. hasseltii	99.88	96	PP975131
3	*C. griseum* PQ728272	*C. griseum*	*C. griseum*	99.88	100	NC_017882
			C. hasseltii	99.87	92	PP975131
4	*C. hasseltii* PP975131	*C. griseum*	*C. hasseltii*	99.81	100	JQ519066
			C. griseum	99.90	100	NC_017882
5	*C. indicum* PP975132	*C. indicum*	*C. indicum*	100	100	JQ519067
6	*C. indicum* PP975133	*C. indicum*	*C. indicum*	100	100	JQ519067
7	*C. indicum* PP975134	*C. indicum*	*C. indicum*	100	100	JQ519067
8	*C. punctatum* PP975136	*C. punctatum*	*C. punctatum*	99.71	100	JQ519064
9	*C. punctatum* PP975137	*C. punctatum*	*C. punctatum*	100	100	MT241400
10	*C. punctatum* PP975138	*C. punctatum*	*C. punctatum*	99.90	100	MT241400

Discussion

The first dorsal fin morphology among *Chiloscyllium* species in this study revealed distinct shapes. The unique concave trailing edge of the first dorsal fin was found in *C. punctatum* while other species showed a straight or slightly convex trailing edge on the first dorsal fin. In the latter group, *C. indicum* and *C. plagiosum* can be distinguished by distinct geomorphic features and a color pattern present in both the juvenile and adult stages. These two species likely represent a slender, elongated dorsal fin shape; however, a previous study (Ahmed *et al.*, 2019; Das *et al.*, 2022) suggests that the group of *C. arabicum* and *C. burmensis* have a straight trailing edge. These species are distinct from other straight-edged species because of their lack of color pattern. The grouping of *C. hasseltii* and *C. griseum* was consistent with their morphological characteristics, as adult *C. hasseltii* closely resembled adult *C. griseum*, but they could be distinguished by morphometric measurements and juvenile color patterns (Dingerkus and DeFino, 1983; Masstor*, et al.*, 2014). Differences in the first dorsal fin provided further distinction, as *C. hasseltii* had a lower height and shorter inner margin than *C. griseum*, with a straight trailing edge in *C. hasseltii* and a slightly convex trailing edge in *C. griseum*.

Differences in the trailing-edge morphology of the first dorsal fin among *Chiloscyllium* species aligned with the evolutionary relationships suggested by the *COI* tree topology. The position of *C. punctatum* as basal species to other *Chiloscyllium* species was revealed in this study and by Vélez-Zuazo and Agnarsson (2011) corresponded with the presence of the unique concave trailing edge of the first dorsal fin. A similar pattern was also revealed in the *ND2* phylogenetic tree, but the tree topology based on this gene showed slight differences, possibly owing to fewer numbers of taxon samples. Phylogenetic analysis of *COI* sequences revealed that the shape of the first dorsal fin may be another key morphological trait that reflects divergence within *Chiloscyllium*. Although there was a mix-up of *C. griseum* and *C. hasseltii* in the same clade because they are evolutionary related, the difference in fin morphology between these two species was clear. The differences in fin height and trailing-edge curvature between *C. hasseltii* and *C. griseum* may reflect adaptations to different environments, potentially influencing swimming efficiency, predation avoidance, and mating behavior (Hoffmann*, et al.*, 2020; Hoffmann and Porter, 2019; Lingham-Soliar, 2005; Sumikawa *et al.*, 2024; Wilga and Lauder, 2001; Wilga and Lauder, 2000). The observed monophyletic grouping of *C. hasseltii* and *C. griseum* may not support their classification as a single species.

Accurate species identification can lead to improvement in studies on the evolutionary relationships of organisms, as morphological characteristics often relate to the evolution of species. The external morphology is complex in

identifying intraspecific variations or minor differences between interspecific variations. The differences in the morphology of the early life stages are more difficult to identify than in adults. While DNA-based identification methods can identify species when morphological characteristics are not available, determine any life stage, and distinguish both intraspecific and interspecific variation, including cryptic species and cases of phenotypic plasticity (Antil *et al.*, 2023; Teletchea, 2009).

Acknowledgements

The author appreciates the assistance of the Department of Fisheries, Thailand and Penchan Laongmanee for dedicating their time and facilitating the collection of samples for the study. We would like to thank Phureerat Bunrot for their illustration of the bamboo sharks, Nattida Srinun and Titirat Meejun for their assistance in taking pictures of the shark's first dorsal fin, Manutsawee Anantiyo for taking the time to conduct the morphometric measurement of the first dorsal fin. This research was funded by King Mongkut's Institute of Technology Ladkrabang, Thailand [KREF016518] and the National Research Council of Thailand (NRCT) [NRCT, N25A650485]. This research was approved by the Animal Care and Use Committee at King Mongkut's Institute of Technology Ladkrabang, Thailand (Approval no. ACUC-KMITL/2023/016).

Conflicts of interest

The authors declare no conflict of interest.

References

Ahmed, M. S., Chowdhury, N. Z., Datta, S. K. and Zhilik, A. A. (2019). New geographical record of the Burmese bamboo shark, *Chiloscyllium burmensis* (Orectolobiformes: Hemiscylliidae), from Bangladesh waters. Thalassas: An International Journal of Marine Sciences, 35:347-350.

Altschul, S. F., Madden, T. L., Schäffer, A. A., Zhang, J., Zhang, Z., Miller, W. and Lipman, D. J. (1997). Gapped BLAST and PSI-BLAST: a new generation of protein database search programs. Nucleic Acids Research, 25:3389-3402.

Antil, S., Abraham, J. S., Sripoorna, S., Maurya, S., Dagar, J., Makhija, S., Bhagat, P., Gupta, R., Sood, U. and Lal, R. (2023). DNA barcoding, an effective tool for species identification: a review. Molecular biology reports, 50:761-775.

Arai, T. and Azri, A. (2019). Diversity, occurrence and conservation of sharks in the southern South China Sea. PLoS One, 14:e0213864.

Arunrugstichai, S., True, J. D. and White, W. T. (2018). Catch composition and aspects of the biology of sharks caught by Thai commercial fisheries in the Andaman Sea. Journal of Fish Biology, 92:1487-1504.

Cole, N. J. and Currie, P. D. (2007). Insights from sharks: evolutionary and developmental models of fin development. Developmental Dynamics, 236:2421-2431.

Compagno, L. J. V. (2001). Sharks of the world: An annotated and illustrated catalogue of shark species known to date, Food and Agriculture Organization of the United Nations, Rome, Italy.

Cooper, J. A., Pimiento, C., Ferrón, H. G. and Benton, M. J. (2020). Body dimensions of the extinct giant shark Otodus megalodon: a 2D reconstruction. Scientific Reports, 10:14596.

Das, B. K., Bhakta, D., Meetei, W. A., Solanki, J. K., Sahoo, A. K., Kumar, L. and Samanta, S. (2022). First report of near threatened Arabian carpetshark, *Chiloscyllium arabicum* Gubanov, 1980, from Narmada Estuary, India. National Academy of Sciences Letters, 45:155-159.

Dharmadi, F. and Satria, F. (2015). Fisheries management and conservation of sharks in Indonesia. African Journal of Marine Science, 37:249-258.

Dingerkus, G. and DeFino, T. C. (1983). A revision of the orectolobiform shark family Hemiscyllidae (Chondrichthyes, Selachii). Bulletin of the AMNH, 176:6-35.

DoA (2009). National plan of action for the conservation and management of sharks in the Philippines. Retrieved from https://faolex.fao.org/docs/pdf/phi208143.pdf

Dulvy, N. K., Pacoureau, N., Rigby, C. L., Pollom, R. A., Jabado, R. W., Ebert, D. A., Finucci, B., Pollock, C. M., Cheok, J. and Derrick, D. H. (2021). Overfishing drives over one-third of all sharks and rays toward a global extinction crisis. Current Biology, 31:4773-4787.e4778.

Elliott, A. C. and Woodward, W. A. (2014). IBM SPSS by example: A practical guide to statistical data analysis, Sage Publications, Singapore.

Hoffmann, S. L., Buser, T. J. and Porter, M. E. (2020). Comparative morphology of shark pectoral fins. Journal of Morphology, 281:1501-1516.

Hoffmann, S. L. and Porter, M. E. (2019). Body and pectoral fin kinematics during routine yaw turning in bonnethead sharks (*Sphyrna tiburo*). Integrative Organismal Biology, 1:obz014.

IUCN (2024). *Chiloscyllium*. Retrieved from https://www.iucnredlist.org/search?query=Chiloscyllium&searchType=species

Klangnurak, W., Arunrugstichai, S., Manopawitr, P. and Krajangdara, T. (2023). DNA-based species identification of shark fins traded in thai markets. Conservation Genetics, 24:537–546.

Klingenberg, C. P. (2011). MorphoJ: an integrated software package for geometric morphometrics. Molecular Ecology Resources, 11:353-357.

Krajangdara, T., Vidthayanon, C., Ali, A., Khiok, A. L. P., Sumontha, M., Rodpradit, S., Chansue, N. and Haetrakul, T. (2022). The Cartilaginous fishes of Thailand adjacent waters, Wanida karnpim, Chaing Mai, Thailand.

Lingham-Soliar, T. (2005). Dorsal fin in the white shark, *Carcharodon carcharias*: a dynamic stabilizer for fast swimming. Journal of Morphology, 263:1-11.

Masstor, N. H., Samat, A., Nor, S. M. and Md-Zain, B. M. (2014). Molecular Phylogeny of the Bamboo Sharks (*Chiloscyllium* spp.). Biomedical Research International, 2014:213896.

Naylor, G. J. P., Caira, J. N., Jensen, K., Rosana, K. A. M., White, W. T. and Last, P. R. (2012). A DNA Sequence–Based Approach To the Identification of Shark and Ray Species and Its Implications for Global Elasmobranch Diversity and Parasitology. Bulletin of the American Museum of Natural History, 367:1-262.

Richterich, P. (2004). CodonCode Aligner Version 1.2 Released. Genetics in Medicine, 6:162-163.

Rohlf, F. J. (2021a). tpsDig2. Version 2.32. Retrieved from http://www.sbmorphometrics.org

Rohlf, F. J. (2021b). tpsUtil. Version 1. 82. Retrieved from http://www.sbmorphometrics.org

Sambrook, J., Fritsch, E. F. and Maniatis, T. (1989). Molecular cloning: a laboratory manual, Cold Spring Harbor Laboratory Press Cold Spring Harbor, New York, USA.

SEAFDEC (2017). Report of regional sharks data collection 2015 to 2016: Results from data collection in sharks project participating countries. South East Asian Fisheries Development Center. Retrieved from https://repository.seafdec.org/handle/20.500.12066/1270

Sternes, P. C., Schmitz, L. and Higham, T. E. (2024). The rise of pelagic sharks and adaptive evolution of pectoral fin morphology during the Cretaceous. Current Biology, 34:2764-2772.

Sumikawa, H., Naraoka, Y., Obayashi, Y., Fukue, T. and Miyoshi, T. (2024). Fluid dynamic properties of shark caudal fin morphology and its relationship to habitats. Ichthyological Research, 71:294-304.

Tamura, K., Stecher, G. and Kumar, S. (2021). MEGA11: molecular evolutionary genetics analysis version 11. Molecular Biology and Evolution, 38:3022-3027.

Teletchea, F. (2009). Molecular identification methods of fish species: reassessment and possible applications. Reviews in Fish Biology and Fisheries, 19:265-293.

Vélez-Zuazo, X. and Agnarsson, I. (2011). Shark tales: a molecular species-level phylogeny of sharks (Selachimorpha, Chondrichthyes). Molecular Phylogenetics and Evolution, 58:207-217.

Ward, R. D., Zemlak, T. S., Innes, B. H., Last, P. R. and Hebert, P. D. (2005). DNA barcoding Australia's fish species. Philosophical Transactions of the Royal Society B: Biological Sciences, 360:1847-1857.

Weigmann, S. (2012). Contribution to the taxonomy and distribution of six shark species (Chondrichthyes, Elasmobranchii) from the Gulf of Thailand. International Scholarly Research Notices, 2012:860768.

Weigmann, S. (2016). Annotated checklist of the living sharks, batoids and chimaeras (Chondrichthyes) of the world, with a focus on biogeographical diversity. Journal of Fish Biology, 88:837-1037.

Wilga, C. D. and Lauder, G. V. (2000). Three-dimensional kinematics and wake structure of the pectoral fins during locomotion in leopard sharks *Triakis semifasciata*. Journal of Experimental Biology, 203:2261-2278.

Wilga, C. D. and Lauder, G. V. (2001). Functional morphology of the pectoral fins in bamboo sharks, *Chiloscyllium plagiosum*: Benthic vs. pelagic station-holding. Journal of Morphology, 249:195-209.

(Received: 13 October 2025, Revised: 16 January 2026, Accepted: 15 April 2026)